Impact of Vehicle Headlights Radiation Pattern on Dynamic Vehicular VLC Channel

F. M. Alsalami, N. Aigoro, A. A. Mahmoud, Z. Ahmad, P. A. Haigh, O. C. L. Haas, and S. Rajbhandari*

Abstract

This paper develops a statistical large-scale fading (path loss) model of a dynamic vehicular visible light communication (VVLC) system. The proposed model combines the impact of inter-vehicle spacing and the radiation intensity distribution as a function of the irradiance angle which changes with the traffic conditions. Three models (Lambertian, Gaussian and empirical) are utilized to examine the impact of vehicles headlights radiation pattern on the statistical path loss of VVLC system. The analytical model of channel path loss is validated by Monte Carlo simulation with the headlight model simulated with a raytracing software. The path loss values of the Gaussian model differ by 2 dB compared to the Lambertian model, irrespective of the traffic conditions while it differs by 24.6 dB during late night and 8.15 dB during rush hours compared to the empirical model of a Toyota Altis headlight. This variation shows that the radiation intensity distribution should be modelled for each vehicle's headlights from each manufacturer to ensure accurate VVLC channel model. The proposed Gaussian model provides a close approximation to describe such radiation pattern and can easily be adapted to model for different manufacturers' headlights.

Vehicle to vehicle (V2V) communication, visible light communication (VLC), outdoor channel model, Statistical communication channel model.

1 Introduction

Intelligent transport systems (ITS) provide solutions to many transportation challenges by the availability of vehicular communication [1]. Vehicular visible light communication (VVLC) offers a complementary solution by exploiting the license-free visible spectrum and hence reducing co-band interference and free the radio frequency (RF)-spectrum for other applications [1, 2].

VVLC maintains connectivity using vehicles' headlight and taillight [2]. These optical devices are directional with an asymmetrical radiation pattern [3–7]. Although the directional nature of optical devices limits the interference among other light sources even in the presence of a high density of vehicles [2], it makes the VVLC link geo-spatial dependent. In addition, the dynamic nature of the traffic changes the geometry of the VVLC link. Therefore, modelling VVLC channel should consider both the radiation pattern of the vehicles' headlights and the dynamic nature of the traffic conditions.

The Lambertian model has been commonly used to describe the symmetrical radiation pattern of light-emitting diode (LED) based sources for indoor environments [8, 9]. In VVLC systems, the Lambertian model has been used to study VVLC channel [1, 2]. However, the ECE R112 regulations, enforce asymmetric radiation pattern designs for low-beam lamps, which are used when vehicles are within a safe stopping distance to reduce the intensity of light directed towards drivers on the opposite lanes [10]. The work reported in [11] considered the radiation patterns of tungsten-halogen lamps to study the VVLC channel model. However, LED lamps are better suited for VVLC as they can support high-speed communication. A comparison between the path loss obtained by the Lambertian model and a simulated model of the asymmetric radiation pattern was provided in [5]. The study simulated the radiation pattern of low-beam headlights (Philips Luxeon Rebel white LED) using a non-sequential raytracing software tool. This study shows that the Lambertian model underestimates the path loss values. The gap between the path loss values of the Lambertian model and the simulated model was justified by the underestimation of reflection from the road surface. However, this is not an issue for VVLC, because the reflection from the road surface has minimal effect due to the low reflectivity values of asphalt (less than 0.3 in its best-case scenario [12, 13]).

The experimental work in [14] provided measurements of VVLC channel path loss using a 2017 Ford Mondeo multibeam headlight. However, the maximum transmission range was limited to 25 m as the experiment was done in a parking garage which does not mirror the realistic scenario involving dynamic traffic. The study in [15] used raytracing method to simulate an Audi R8 headlamp to study the channel impulse response (CIR) of VVLC for different streets scenarios. However, the study did not provide an analytical CIR model which can be used to design a robust communication link. In addition, the study did not consider variable traffic conditions.

The study in [4] considered a small-scale VVLC channel fading using realistic headlight radiation pattern for the Toyota Altis headlamp. This study provided measurements of the time variation characteristics of the channel, but it did not provide a reliable path loss channel model expression that can be used to design a VVLC link. The study also did not consider traffic flow and vehicles density. Similarly, the work in [6] characterized the radiation pattern of the 2015 Toyota Corolla Altis headlight and taillight to study the difference between the received power over the incoming and outgoing links. The measurement campaign was conducted in a large open space at night to minimize the ambient noise from other light sources. The

*FMA, NA, AAM, ZA, OCLH: Coventry University, CV1 5FB, UK, (E-mails: (alsallaf, aigoron, mahmou14)@uni.coventry.ac.uk, and (ab7175, o.haas)@coventry.ac.uk) PAH: Newcastle University, NE1 7RU, UK, (E-mails: Paul.Haigh@newcastle.ac.uk) SR: SmartLiFi, UK. (E-mail: sujan@ieee.org).

work in [7] used the radiation pattern measurements reported in [6] to derive a path loss formula which comprises two parts: a) propagation path loss due to distance and b) geometrical path loss due to angle deviation. Likewise, the work in [16] used path loss formula in [7] as a benchmark to compare a proposed VVLC channel model with a simulation channel model. The simulated model used the radiation pattern of the low beam headlight (Philips Luxeon Rebel white LED) using the non-sequential raytracing software tool that was used in [5]. However, the path loss values obtained for the same headlight at the same distances differ e.g. the path loss values are -58 dB and -46 dB for simulated model in [5] and measurements in [16], respectively.

A piecewise Lambertian analytical channel model was proposed and validated based on measurements from a Yamaha Cygnus-X scooter taillight [3]. However, the piecewise Lambertian model is not valid for other types of low-beam and high-beam headlamps [17]. The work in [17] concluded that finding a universal path loss model that can describe the radiation pattern of different designs of vehicles headlights and taillights is difficult and complex. However, the study emphasized the importance of finding such a model to analyse the link budget and predict the performance of the VVLC link.

The studies in [18, 19] modeled the radiation intensity distribution of asymmetrical radiation patterns of different LEDs using a linear combination of Gaussian functions for the indoor environment. The proposed model was found to accurately describe the radiation intensity distribution of asymmetrical radiation patterns LEDs from different manufacturers.

The impact of weather conditions and attenuation due to the scattering effect in the air was modeled and studied in [20, 21]. For example, additional attenuation of 0.7 dB/km, 7.77 dB/km, 10.5 dB/km, 15.96 dB/km and 34.69 dB/km are induced due to clear, haze, thin fog, light fog, and dense fog, respectively [20, 21]. In our previous work [21], we studied the additional attenuation that different weather conditions add to the path loss of VVLC channel. In addition, we studied the impact of reflection from vehicles and other road materials. The results showed that, among the considered surfaces, reflection from vehicles has a significant effect on the path loss because the reflectivity values of other surfaces are comparatively low. Furthermore, the results showed that the path loss values of reflection component are very large compared to the path loss values of the LOS component when a single reflector is considered and decreases significantly in multiple reflections scenario.

1.1 Motivation and Original Contribution

As described in section I, there is a lack of coherent VVLC channel model for a dynamic VVLC system which takes into account the radiation pattern of vehicles' headlights under realistic traffic conditions. This study considers the large-scale fading because it dominates VVLC performance. This is due to the modest effect of small-scale fading presented by the time stationary property and dispersion parameters of the VVLC channel [4, 22]. The experimental measurements in [4] and our previous theoretical study in [22], which considered the dynamic nature of traffic conditions during different time of the day, showed that a VVLC channel has flat and slow fading characteristics at different traffic conditions. Therefore, in this study, we focus on the large-scale fading (path loss) model which has particular importance in accurately estimating the link budget, the outage probability and capacity of the VVLC channel [23, 24]. We address the lack of VVLC channel model considering various radiation patterns and dynamic traffic conditions. The main contributions of this work are as follows:

- Propose an analytical model that can describe the statistical path loss of the VVLC channel. To the authors' knowledge, this is the first model that considers the impact of the asymmetric radiation pattern of the vehicles' headlights combined with the effect of dynamic variation of vehicles movement pattern due to varying traffic conditions. The model relies on traffic measurements collected from the M42 and M6 highways in the UK.
- Model the radiation intensity of vehicles headlights with a series of Gaussian functions. The Philips LUXEON® Rebel which is commonly utilised for automotive applications [25] is used as an example of a practical vehicle's headlight.
- The proposed model is validated by Monte Carlo simulation where the light transmission is computed using a non-sequential ray-tracing software.
- Compared the statistical path loss distributions for three different radiation pattern models and quantified the results demonstrating the effect of the radiation pattern.

The rest of the paper is organized as follows: the CIR is presented in section II. The dynamic traffic conditions are analyzed in section III. The headlight radiation pattern models are described in section IV. The numerical results are discussed in section V and conclusions are presented in section VI.

2 Channel impulse response

The radiation pattern of the vehicle's headlight has rotationally asymmetrical angular distribution [17]. The radiation intensity distribution depends on the manufacturer design parameters such as the number of LEDs, alignments of the LEDs, existence/absence of optics and reflection shields [17]. Therefore, if the three-dimensional radiation intensity distribution of an asymmetrical radiation pattern is $I(\phi, \Phi)$ then the radiation irradiance distribution at distance D, also called illuminance (W/m^2), is given by [11, 18, 26]:

$$E(\phi, \Phi, \psi) = \frac{I(\phi, \Phi)\cos(\psi)}{D^2} \tag{1}$$

Table 1: Log-normal distribution parameters that describe the inter-vehicle spacing during rush hours and late night hours.

Time	Mean (m)	μ_s	σ_s	μ_d	σ_d
0:00-3:00	48.72	3.88	0.09	3.90	0.08
12:00-15:00	12.37	2.51	0.12	2.59	0.11

where ϕ is the irradiance azimuth (horizontal) angle, Φ is the elevation (vertical) angle, ψ is the incident angle at the receiver and D is the inter-vehicle spacing.

If the receiver uses a photodiode (PD) with an active aperture area of A_r, an optical filter with a gain of $T_s(\psi)$ and a concentrator with a gain of $g(\psi)$, then the CIR is given by [17]:

$$h(t) = \frac{I(\phi,\Phi)}{D^2} A_r T_s(\psi) g(\psi) \cos(\psi) \delta\Big(t - \frac{D}{c}\Big) \tag{2}$$

where t represents the propagation time, c is the speed of light, D/c is the propagation delay of the signal.

Assuming that the optical filter and the concentrator have unit gain, the alignment between vehicles heading is maintained, i.e. $\phi = \psi$, then the DC gain of the channel H(0) is given by:

$$H(0) = \frac{A_r I(\phi,\Phi)}{D^2} \cos(\phi) \tag{3}$$

The empirical study in [4] considered the impact of the vertical movement of vehicles, due to road surface irregularities, on the path loss and received power variation. The study showed that vertical movements cause a rapid increase (< 5 dB) in the received power which last for less than 0.5 s. Therefore, without loss of generality, it is assumed that the PD is aligned with the light source for most of the time. Hence, the elevation angle Φ can be considered as a constant and radiation intensity distribution can be reduced to $I(\phi)$.

The path loss (channel gain in decibels (dB)), therefore, is given by:

$$P_L = 10\log(A_r) + 10\log(I(\phi)\cos(\phi)) - 20\log(D) \tag{4}$$

The P_L depends on the geometrical dimensions of the communication link D and ϕ which changes due to the dynamic nature of traffic conditions. In the next section, we study the geometrical changes in the communication link due to traffic.

3 Dynamic traffic conditions

Due to the dynamic nature of traffic conditions, the path loss P_L at any time instance is random because the geometrical dimensions of the communication link D and ϕ are changing. Hence, the path loss P_L depends on the road traffic conditions, traffic flow (veh/h), vehicles density (veh/m) and vehicle speed (m/h) [27]. The inter-vehicle spacing D distribution varies with the traffic flow, which also varies with time [28].

We use data collected using a combination of multiple-loop sensors; 318 and 154 bridge-mounted sensors on the M42 and M6 motorways in the UK, respectively. The data was collected from the M42 and M6 on the days (21, 24 and 28) of November 2017 and (6, 7 and 8) of December 2017, respectively. From these data, we extract the traffic flow variation and inter-vehicle spacing D variation over each 24 hour period [29].

The average traffic flow variation and inter-vehicle spacing variation during the day are illustrated in Fig. 1(a). The figures show that the traffic flow exceeds 1000 veh/h from 6:00 to 19:00. Accordingly, D has the lowest values during this period. Therefore, we use a sample time window between 12:00 and 15:00 to study the rush hours traffic scenario when the traffic flow exceeds 1000 veh/h. On the other hand, the figures show that the traffic flow is below 500 veh/h at 23:00-7:00. Hence, D has the largest values during this period of the day. Therefore, we use a sample time window between 0:00 and 3:00 to study the late hours traffic scenario when the traffic flow is below 500 veh/h.

Random variation of the inter-vehicle spacing is described using different distributions such as exponential, normal and log-normal [28, 30]. From the traffic measurements, the cumulative density functions (CDF) of inter-vehicle spacing during the rush hours 12:00-15:00 and late-night hours 0:00-3:00 in Fig. 1(b) show that a log-normal distribution with parameters μ_s and σ_s gives a good fit to the inter-vehicle spacing D:

$$P_D(d) = \frac{1}{\sigma_s\sqrt{2\pi}} \frac{1}{d} exp\Big(-\frac{(\ln(d)-\mu_s)^2}{2\sigma_s^2}\Big) \tag{5}$$

The values of parameters μ_s and σ_s at different period of the day are given in Table 1. The log-normal distribution is a realistic scenario which accounts for the spacing between two consecutive vehicles and the speed limits of the road. The random distribution that describes the path loss P_L in (4) combines the effect of the variation of D and the inter-vehicular angle deviation ϕ which depends on the angular distribution of the radiation pattern of the light source.

In the following section, we study the impact of vehicles headlight radiation pattern model on the statistical distribution of VVLC path loss.

4 Headlight radiation pattern models

In this work, we use three different models to examine the impact of the luminous intensity distribution and effects of the asymmetrical pattern on the statistical distribution of vehicular channel path loss. These models include a) the Lambertian model which is conventionally used to describe the symmetrical angular distribution of the radiation intensity patterns, b) a series of Gaussian functions to describe the asymmetrical angular distribution of the radiation intensity patterns and c) the empirical path loss model described in [7] for the asymmetric radiation intensity pattern of a 2015 Toyota Altis low-beam headlamp.

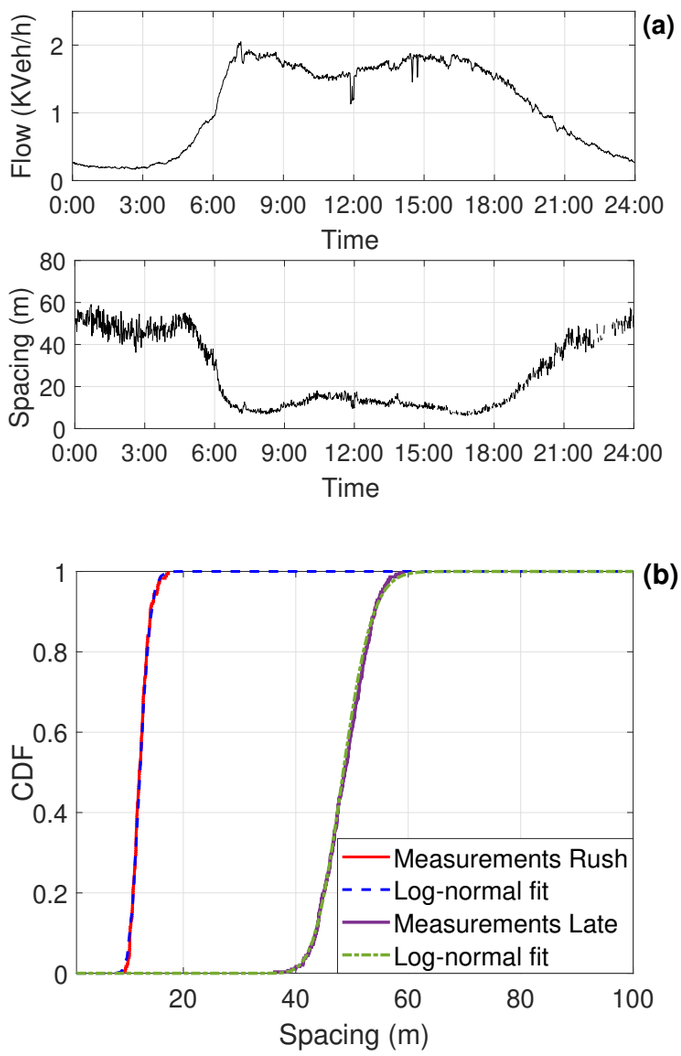

Figure 1: a) Traffic flow variation and inter-vehicle spacing variation during the day; b) CDF of inter-vehicle spacing during the rush and late-night hours

4.1 The Lambertian angular distribution model

The Lambertian radiation model is conventionally used to describe the symmetrical angular distribution of the radiation intensity pattern of a LED light source. The radiation intensity distribution $I(\phi)$ of a Lambertian source is given by:

$$I(\phi) = \frac{(m+1)}{2\pi} \cos^m(\phi) \tag{6}$$

where $m = \frac{-0.6931}{\ln(\cos(\Psi_{1/2}))}$ is the Lambertian order and $\Psi_{1/2}$ is the half-power angle of the radiation. For a Lambertian source, the path loss in (4) can be simplified to:

$$P_L = 10\log(A_r(m+1)) - 10\log(2\pi) - 20\log D + 10(m+1)\log\cos(\phi) \tag{7}$$

Considering the log-normal distribution of D in (5), the terms $10\log(A_r(m+1)) - 10\log(2\pi) - 20\log D$ have normal distribution [31] with standard deviation $\sigma_m = 20\sigma_s/\ln(10)$ and mean $\mu_m = 10\log(A_r(m+1)/2\pi) - 20(\mu_s/\ln(10))$.

The azimuth angle ϕ depends on the variation of the lateral offset between following vehicles. Finding a realistic statistical distribution, that describes the distribution of the lateral offset between vehicles and hence the azimuth angle, depends on many variables including traffic volume, types and width of vehicles, lane width, vehicles speed and maneuvering [20, 32]. Experimental works obtained different distributions to describe the random distribution of the lateral offset between vehicles in reference to a specific variable [32–34]. To average out the aforementioned variable and account the effect of the radiation pattern exclusively as a function of ϕ, the angle is assumed to be uniformly distributed $\phi \sim U(0, \phi_o)$ [20]. The cosine distribution is given by [31]:

$$f_{Z_\phi}(z_\phi) = \frac{1}{\phi_o\sqrt{1-z_\phi^2}} \qquad \cos(\phi_o) < z_\phi < 1 \tag{8}$$

Now, applying the principles of random variable transformation, the term $10(m+1)\log\cos(\phi)$ in (7) can be expressed as:

$$f_Y(y) = \frac{1}{g\phi_o\sqrt{e^{-2y/g}-1}} \qquad 0 < y < 10(m+1)\log\cos(\phi_o) \tag{9}$$

where $g = 10(m+1)\log e$.

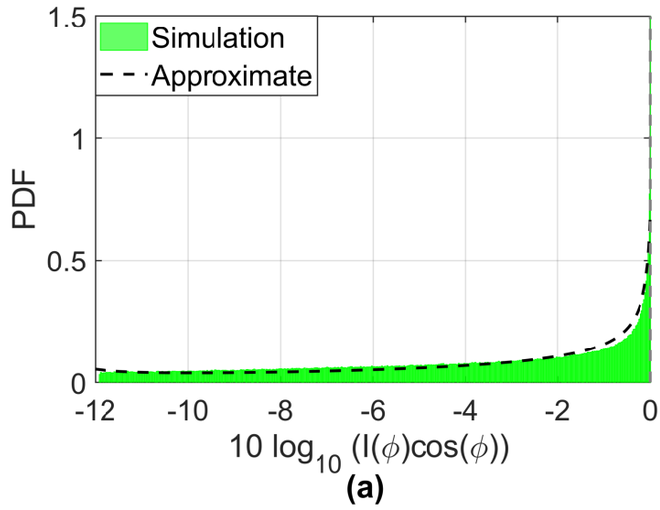

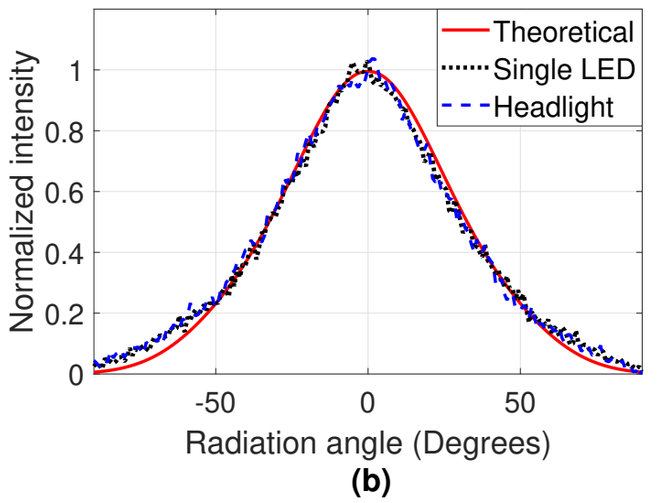

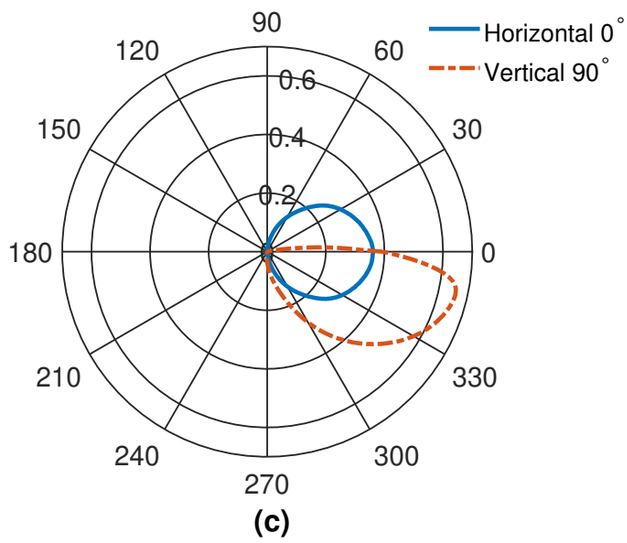

Figure 2: a) The numerical evaluation of the Gaussian radiation pattern model PDF term when $\phi_o = 60°$; b) Normalised single LED and headlight Gaussian intensity; c) horizontal/vertical headlight radiation patterns.

Hence, the statistical distribution of path loss in (7) is found by the convolution of the distribution of the inter-vehicle spacing and the log-cosine distribution in (9) which is given by:

$$P_L(x;\mu_m,\sigma_m) = \frac{1}{g\phi_o\sigma_m\sqrt{2\pi}} \int_{\alpha_m}^{0} \frac{\exp\left(-\frac{(x-y-\mu_m)^2}{\sigma_m^2}\right)}{\sqrt{e^{-2y/g}-1}}\, dy \tag{10}$$

where $\alpha_m = 10(m+1)\log(\cos(\phi_o))$.

4.2 The Gaussian angular distribution model

It was reported in [18, 19] that the asymmetrical luminous intensity distribution can be described by a series of Gaussian functions as:

$$I(\phi,\Phi)=\sum_i g1_i \exp\Big(-\ln(2)\Big(|\phi|-g2_i\Big)^2\Big(\frac{\cos^2\Phi}{(g3_i)^2}+\frac{\sin^2\Phi}{(g4_i)^2}\Big)\Big) \tag{11}$$

where ($g1_i$, $g2_i$, $g3_i$, and $g4_i$) are coefficient identified by linear regression.

According to [18], two to three terms of Gaussian functions can describe the radiation distribution with sufficient accuracy. Therefore, the horizontal distribution can be re-written as:

$$I(\phi)=g1_1\exp\Big(-\ln(2)\Big(\frac{|\phi|-g2_1}{g3_1}\Big)^2\Big)+g1_2\exp\Big(-\ln(2)\Big(\frac{|\phi|+g2_2}{g3_2}\Big)^2\Big) \tag{12}$$

The intensity distribution $I(\phi)$ is given by a combination of two shifted Gaussian functions, which can approximate a sinusoidal function [35]. Using numerical evaluation, it can be shown that the term $I(\phi)\cos(\phi)$ in (4) can closely fit $c_1\cos(c_2\phi)+c_3$, where the coefficients (c_1,c_2 and c_3) are identified numerically. Hence, the distribution of the term $10\log(I(\phi)\cos(\phi))$ in (4) can be approximately given by:

$$f_Y(y)=\frac{e^{y/a}}{a\ c_2\ \phi_o\sqrt{c_1^2-(e^{y/a}-c_3)^2}} \qquad 0<y<c_4 \tag{13}$$

where $a=10/\ln(10)$ and c_4 is a boundary constant, which is identified numerically.

Fig. 2(a) shows a numerical evaluation of the radiation pattern term when $\phi_o=60°$. In this case, the numerical values of coefficients $c_1=0.48$, $c_2=1/3$, $c_3=0.534$ and $c_4=11.9$ provide an approximate fit with a mean squared error of 0.25. The combination of other terms $10\log(A_r)-20\log D$ of (4) has a normal distribution with a standard deviation of $\sigma_n=20\sigma_s/\ln(10)$ and mean of $\mu_n=10\log(A_r)-20\frac{\mu_s}{\ln(10)}$. The distribution of path loss is given by the convolution between the normal distribution of the inter-vehicle spacing and the distribution given in (13). This convolution gives the following distribution:

$$P_L(x;\mu_n,\sigma_n)=\frac{1}{a\ c_2\ \phi_o\sigma_n\sqrt{2\pi}}\int_{c_4}^{0}\frac{exp\Big(-\frac{(x-y-\mu_n)^2}{\sigma_n^2}-\frac{y}{a}\Big)}{\sqrt{c_1^2-(e^{y/a}-c_3)^2}}\,dy \tag{14}$$

4.3 Empirical asymmetric radiation pattern of Toyota Altis Headlight

The empirical study in [7] considered the asymmetric radiation intensity pattern of the low-beam headlamp to provide a path loss formula, which is given by:

$$P_L[dB]=\alpha+\delta-10\beta\log\Big(D+1\Big)+\epsilon\cos\Big(\frac{2\pi(\theta+90)}{\omega}\Big) \tag{15}$$

where θ the incident angle, $\alpha=695.3$, $\delta=-717.3$ (accounts for dBm to dB conversion), $\beta=4.949$, $\epsilon=63.13$ and $\omega=173$. Considering that the inter-vehicle spacing has a log-normal distribution with a mean value $>>1$, then the term $10\beta\log\Big(D+1\Big)$ follows a normal distribution which is approximately expressed as [31]:

$$P_L(x;\mu_d,\sigma_d)=\frac{1}{\sigma_d\sqrt{2\pi}}exp\Big(-\frac{(x-\mu_d))^2}{2\sigma_d^2}\Big) \tag{16}$$

where both the standard deviation σ_d and the mean μ_d are affected by the constant shift of $D+1$, which are given by $\mu_d+\sigma_d^2/2=\ln(1+e^{\mu_s+\sigma_s^2/2})$. The numerical values of σ_d and μ_d are given in Table 1.

Similar to (8), when $\theta\ \sim\ U(0,\theta_o)$, the term $\epsilon\cos\Big(\frac{2\pi(\theta+90)}{\omega}\Big)$ is given by a linear transformation of the cosine distribution:

$$f_{Z_\theta}(z_\theta)=\frac{\omega}{2\pi\theta_o\sqrt{\epsilon^2-z_\theta^2}} \qquad \alpha_{cmin}<z_\theta<\alpha_{cmax} \tag{17}$$

where $\alpha_{cmin}=\epsilon\cos(2\pi(\theta_o)/\omega)$ and $\alpha_{cmax}=\epsilon\cos(2\pi(\theta_o+90)/\omega)$.

Therefore, the distribution of the path loss given in (15) follows a convolution between the normal distribution of the inter-vehicle spacing in (16) and a cosine distribution in (17). This convolution gives the following distribution [31]:

$$P_L(x;\mu_c,\sigma_c)=\frac{\omega}{(2\pi)^{(3/2)}\theta_o\sigma_c}\int_{\alpha_{cmin}}^{\alpha_{cmax}}\frac{\exp\Big(-\frac{(x-y-\mu_c)^2}{\sigma_c^2}\Big)}{\sqrt{\epsilon^2-y^2}}\,dy \tag{18}$$

where the standard deviation $\sigma_c=10\beta\sigma_d/\ln(10)$ and the mean $\mu_c=\alpha-10\beta\mu_d/\ln(10)$.

5 RESULTS and DISCUSSION

To validate the mathematical analysis of the Gaussian model of a LED Philips LUXEON® Rebel presented in section III.B, a raytracing software OpticStudio® is utilized with the luminous intensity profile obtained from manufacturer datasheet to obtain the statistical path loss distribution of the VVLC channel. The received power is obtained at distances ranging from 1 m to 100 m (to reflect inter-vehicular distance of rush hour and late night hour) with lateral distance from 0 m to 1 m from both sides of the source. Further

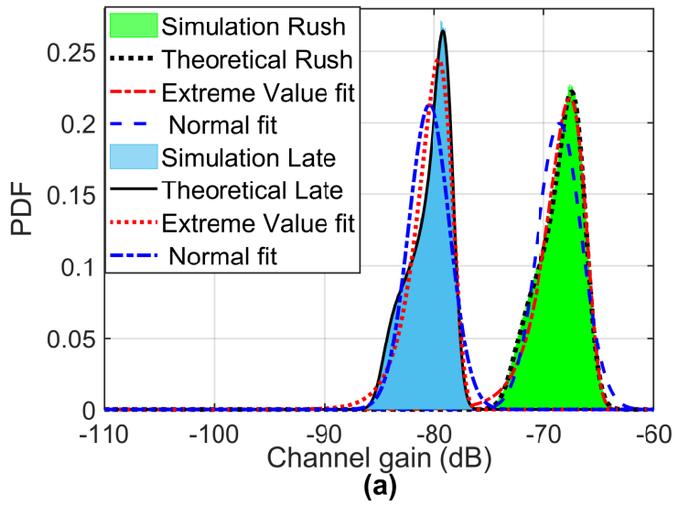

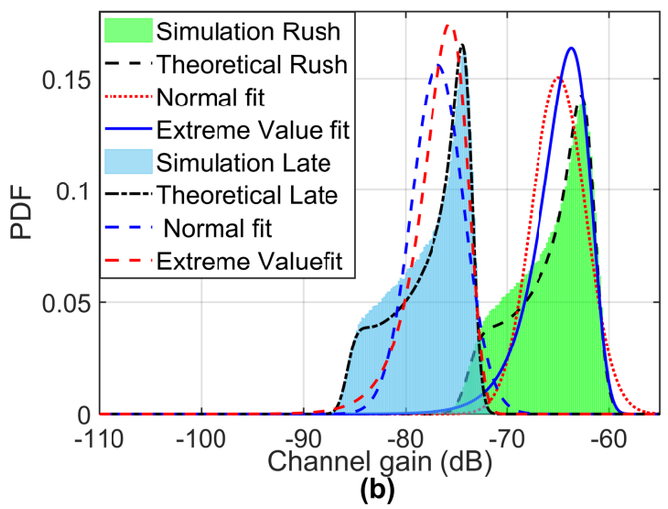

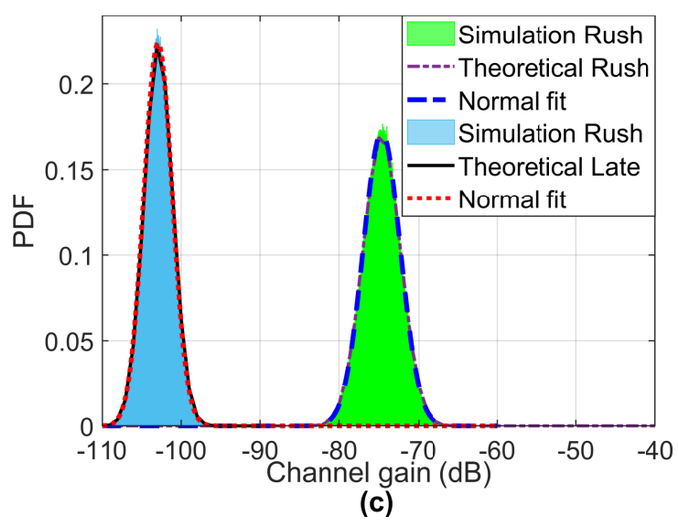

Figure 3: Path loss PDFs for a) Lambertian and b) Gaussian and c) empirical radiation models at 0:00-03:00 (late hours) and 12:00-15:00 (rush hours).

analysis (e.g. path loss and CDF of path loss) is carried out in MATLAB using the data obtained from the raytracing.

First, we use the normalized intensity to find the numerical values of the coefficients $g1_1$, $g1_2$, $g2_1$, $g2_2$, $g3_1$ and $g3_2$ for the headlight pattern as shown in Fig. 2(b). The figure shows that the normalized intensity of the headlight pattern matches the normalized intensity of a single Philips LUXEON® Rebel. This is expected because the receiver is aligned to the horizontal plane 0°. Fig. 2(c) shows that in this plane the intensity has the same pattern for a single LED. Therefore, the numerical coefficients $g1_1$=0.76, $g1_2$=0.11, $g2_1$=0, $g2_2$=45°, $g3_1$=29° and $g3_2$=21° [18, 19] closely fit the normalized intensity of the headlight pattern with a root-mean-square-error (RMSE) value 0.02, verifying that the Gaussian angular distribution model can closely match the radiation pattern of the LED.

Based on these radiation patterns, we studied the dynamic path loss distributions. We assume that the channel gain at any time instant is random and depends on inter-vehicle spacing as well as irradiance azimuth angle. Monte Carlo (MC) simulation of 10^6 iterations is used to study the dynamic behaviors of the system under study based on the statistical model described in Section IV. In the simulation, concentrator

Table 2: Summary of mean and variance values of the statistical path loss distributions.

Time	Model	mean value (dB)	variance
0:00-3:00	Lambertian	-79.6	3.7
	Empirical	-102.8	3.2
	Gaussian	-77.7	13.1
12:00-15:00	Lambertian	-68.6	4.7
	Empirical	-74.7	5.4
	Gaussian	-65.8	14.2

gain of 1 and FOV of 80°. The inter-vehicle distance D has a log-normal distribution with μ_s and σ_s given in Table 1. The angles ϕ and θ are assumed to be uniformly distributed $\phi \sim U(0, 60°)$. The simulation assumed clear weather conditions with negligible additional attenuation. Similarly to the empirical model in [7], the non-line-of-sight (NLOS) reflection from vehicles and road surfaces is not considered and a receiver with an active area of 1 cm^2 is mounted at the same headlights' horizontal plane (i.e. receiver height at 55 cm) [6, 7].

The probability density functions (PDFs) of channel path loss obtained by a) Lambertian b) Gaussian and c) empirical radiation in [7] models at 0:00-03:00 (late hours) and 12:00-15:00 (rush hours) are shown in Fig. 3. The figures demonstrate that the path loss distribution obtained using MC simulation matches with the theoretical analysis given by (10), (14) and (18) for the Lambertian, the Gaussian and empirical radiation models, respectively. The figure shows that the path loss distribution is affected by the variation of inter-vehicle spacing and the radiation pattern distribution. All models show that the path loss values at late hours are higher than values at rush hours. This is expected, as the mean values of the inter-vehicle spacing μ_s and μ_d have larger values at late hours compared to the rush hours as illustrated in Table 1.

It is difficult to evaluate the system performance using the PDFs of the path loss expressed in the integration form in (10), (14) and (18). However, these integration formulas cannot be further simplified or expressed in terms of a finite combination of elementary functions [36, P. 229]. Therefore, Fig. 3 suggests conventional statistical distributions that can fit the obtained path loss distributions. A normal distribution has provided a close approximation to the empirical model path loss because changes in the inter-vehicular distances, described by normal distributions, have a dominant effect. An extreme value distribution has provided a close approximation to the path loss distribution when the Lambertian model is used, particularly at rush hours. This is because, in the Lambertian model, changes in the inter-vehicular distance has a relatively larger effect than changes in the angles ϕ which has cosine distributions. The path loss distribution, when the Gaussian model is used, cannot be described by a conventional distribution because it is affected equally by the changes in the inter-vehicular spacing and the angles ϕ. Hence, this study found that the convolution between a normal distribution and log-cosine distribution in (14) best describes the path loss distribution.

Fig. 4(a) illustrates the CDF of the path loss obtained by raytracing approach and MC simulation using the Gaussian model at 0:00-03:00 and 12:00-15:00. The received power values are used to find the path loss according to the mean and standard deviation of distance distributions in Table 1 and Fig. 1(b). The figure shows that the Gaussian model closely matches the path loss obtained by raytracing and predicts the mean values of the path loss at both periods.

Fig. 4(b) shows the CDFs for path loss of the Lambertian, empirical and Gaussian models. The mean and standard deviation values of the path loss are summarized in Table 2. The figure and table clearly show that mean and standard deviation values of path loss depend on the radiation pattern. The mean path loss is the lowest for the Gaussian model followed by Lambertian and Empirical models. The difference in the path loss is 2 dB between the Gaussian and Lambertian radiation pattern and > 8 dB between Gaussian and Empirical radiation pattern. This difference in the path loss values does not mean that some models are more accurate than others. This difference in path loss values only indicates that path loss is dependent on the radiation pattern. Since different manufactures use different technology and optical systems which significantly affect the radiation pattern, the path loss for VVLC system also varies for different headlamps. In conclusion, the path loss of the empirical model is only applicable for the Toyota Altis low-beam lamp, because it does not accurately describe the path loss of other light sources of a different design and function. The Lambertian model is impractical to describe the asymmetrical radiation pattern of vehicles' sources. The proposed Gaussian model can be adopted to describe the radiation pattern of different vehicles' sources for different manufacturers by adjusting the values of the coefficients $g1_1$, $g1_2$, $g2_1$, $g2_2$, $g3_1$ and $g3_2$.

To study the impact of the radiation pattern on the communication link performance, we examine the bit-error-rate (BER) performance for on-off keying (OOK) modulation scheme. The BER estimate of the system and simulation parameters are given by [11]. Assuming a pseudo-random sequence of 10^6 bits and a transmission rate of 50 Mbps, the estimated BER performances from the comparative statistical analysis for the three path loss models is illustrated in Fig. 4(c). The simulation parameters are given in [11]. The figure shows that to achieve BER=10^{-5} the difference in the required SNR values for Gaussian and Lambertian models is 2 dB at the rush and late hours. The difference in the required SNR for the Lambertian and Empirical models is 18 dB at rush hours and increases to 51 dB at late hours. This is expected because the path loss values for the Gaussian and Lambertian models are close while the path loss values of the Empirical model are significantly higher than the Gaussian and Lambertian models as illustrated in Table 2.

6 Conclusion

In this paper, we developed a statistical path loss model of a dynamic VVLC channel using Lambertian, Gaussian and asymmetrical radiation patterns that model headlamps from different manufacturers. The study shows that the path loss depends on radiation patterns as well as the traffic conditions including traffic flow and inter-vehicular spacing which are dynamically varying. The theoretical analysis confirms

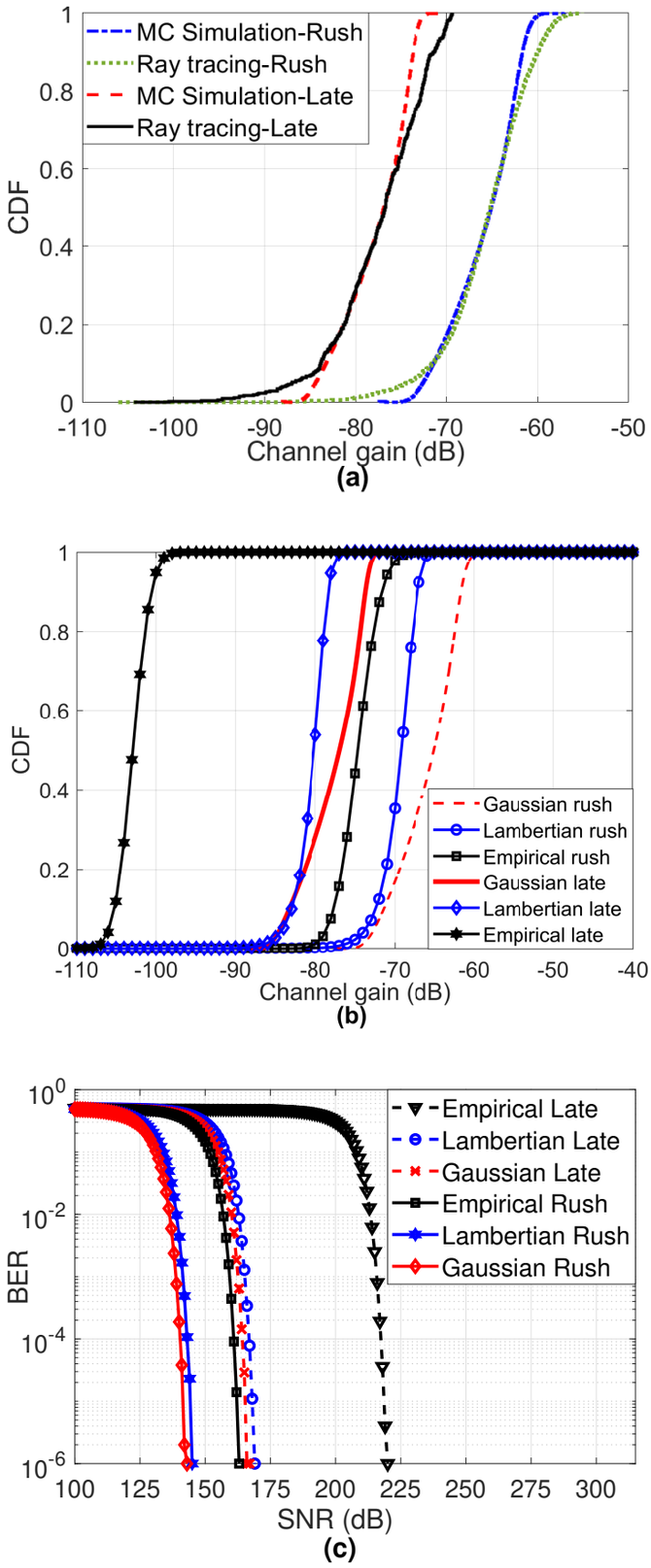

Figure 4: Path loss CDFs at 0:00-03:00 and 12:00-15:00 for (a) Gaussian MC model; (b) Lambertian, Gaussian angular distribution and empirical models; and (c) estimated BER performance of OOK modulation scheme for each of the models at different traffic conditions.

that statistical distribution of the path loss is a convolution of the radiation intensity distribution and the inter-vehicle spacing distribution. The statistical path loss varies significantly depending upon the radiation pattern with a difference of > 8 dB. The Gaussian radiation pattern shows the least path loss followed by Lambertian and asymmetrical pattern. Developing a universal model to describe the radiation pattern for different headlights of different designs and manufacturers is not feasible because radiation patterns from different manufacturers have different features and characteristics. However, finding the radiation intensity distribution of vehicles headlights for each manufacturer is important to model the VVLC channel. The Gaussian model provides a close approximation to describe the radiation pattern which can easily be adopted for different manufacturers.

Acknowledgements

The authors would like to thank Highways England and Mott MacDonald for providing us with traffic data.

References

[1] A. Al-Kinani, J. Sun, C. Wang, W. Zhang, X. Ge, and H. Haas, "A 2-D non-stationary GBSM for vehicular visible light communication channels," *IEEE Trans. Wireless Commun.*, vol. 17, no. 12, pp. 7981–7992, 2018.

[2] J. Chen and Z. Wang, "Topology control in hybrid VLC/RF vehicular Ad-Hoc network," *IEEE Trans. Wireless Commun.*, vol. 19, no. 3, pp. 1965–1976, 2020.

[3] W. Viriyasitavat, S.-H. Yu, and T. Hsin-Mu, "Short Paper : Channel Model for Visible Light Communications Using Off-the-shelf Scooter Taillight," *Proc. 2013 IEEE VNC*, pp. 170–173, 2013.

[4] A. Chen, H. Wu, Y. Wei, and H. Tsai, "Time variation in vehicle-to-vehicle visible light communication channels," in *Proc. 2016 IEEE VNC*, 2016, pp. 1–8.

[5] H. Abuella, F. Miramirkhani, S. Ekin, M. Uysal, and S. Ahmed, "ViLDAR—visible light sensing-based speed estimation using vehicle headlamps," *IEEE Trans. Veh. Technol.*, vol. 68, no. 11, pp. 10 406–10 417, 2019.

[6] Hua-Yen Tseng, Y. Wei, Ai-Ling Chen, Hao-Ping Wu, Hsuan Hsu, and H. Tsai, "Characterizing link asymmetry in vehicle-to-vehicle visible light communications," in *Proc. 2015 IEEE VNC*, 2015, pp. 88–95.

[7] A. Memedi, H. Tsai, and F. Dressler, "Impact of realistic light radiation pattern on vehicular visible light communication," in *Proc. GLOBECOM 2017*, Singapore, 2017, pp. 1–6.

[8] J. Wang, C. Liu, J. Wang, Y. Wu, M. Lin, and J. Cheng, "Physical-layer security for indoor visible light communications: Secrecy capacity analysis," *IEEE Trans. Wireless Commun.*, vol. 66, no. 12, pp. 6423–6436, 2018.

[9] J.-Y. Wang, Q.-L. Li, J.-X. Zhu, and Y. Wang, "Impact of receiver's tilted angle on channel capacity in VLCs," *Electronics Letters*, vol. 53, no. 6, pp. 421–423, 2017.

[10] United Nations, "United Nations Economic Commission for Europe vehicle regulations, Reg. 112-Rev.3," *UN*, no. 9789241565684, Jan. 2013. [Online]. Available: https://www.unece.org/fileadmin/DAM/trans/main/wp29/wp29regs/2013 /R112r3e.pdf

[11] P. Luo, Z. Ghassemlooy, H. L. Minh, E. Bentley, A. Burton, and X. Tang, "Performance analysis of a car-to-car visible light communication system," *Appl. Opt.*, vol. 54, no. 7, pp. 1696–1706, Mar 2015.

[12] W. Adrian and R. Jobanputra, "Influence of pavement reflectance on lighting for parking lots," Portland Cement Association, Skokie, IL, USA, Research and Development information SN2458, 2005.

[13] E. Puttonen, J. Suomalainen, T. Hakala, and J. Peltoniemi, "Measurement of reflectance properties of asphalt surfaces and their usability as reference targets for aerial photos," *IEEE Trans. Geosci. Remote Sens.*, vol. 47, no. 7, pp. 2330 – 2339, Aug. 2009.

[14] A. Uyrus, B. Turan, E. Basar, and S. Coleri, "Visible light and mmWave propagation channel comparison for vehicular communications," in *Proc. 2019 IEEE VNC*, 2019, pp. 1–7.

[15] S. Lee, J. K. Kwon, S.-Y. Jung, and Y.-H. Kwon, "Evaluation of visible light communication channel delay profiles for automotive applications," *EURASIP Journal on Wireless Communications and Networking*, vol. 2012, no. 1, p. 370, 2012.

[16] M. Karbalayghareh, F. Miramirkhani, H. B. Eldeeb, R. C. Kizilirmak, S. M. Sait, and M. Uysal, "Channel modelling and performance limits of vehicular visible light communication systems," *IEEE Transactions on Vehicular Technology*, pp. 1–1, 2020.

[17] L. Cheng, W. Viriyasitavat, M. Boban, and H. Tsai, "Comparison of radio frequency and visible light propagation channels for vehicular communications," *IEEE Access*, vol. 6, pp. 2634–2644, 2018.

[18] I. Moreno and C.-C. Sun, "Modeling the radiation pattern of LEDs," *Opt. Express*, vol. 16, no. 3, pp. 1808–1819, Feb 2008.

[19] J. Ding, C. I, and Z. Xu, "Indoor optical wireless channel characteristics with distinct source radiation patterns," *IEEE Photonics Journal*, vol. 8, no. 1, pp. 1–15, 2016.

[20] Y. H. Kim, W. A. Cahyadi, and Y. H. Chung, "Experimental demonstration of VLC-based vehicle-to-vehicle communications under fog conditions," *IEEE Photonics Journal*, vol. 7, no. 6, pp. 1–9, Dec 2015.

[21] F. M. Alsalami, Z. Ahmad, S. Zvanovec, P. A. Haigh, O. C. Haas, and S. Rajbhandari, "Statistical channel modelling of dynamic vehicular visible light communication system," *Vehicular Communications*, vol. 29, p. 100339, 2021.

[22] F. M. Alsalami, Z. Ahmad, P. A. Haigh, O. Haas, and S. Rajbhandari, "The statistical temporal properties of vehicular visible light communication channel," in *Proc. 12th IEEE/IET CSNDSP*, July 2020.

[23] J. Y. Wang, Y. Qiu, S. H. Lin, J. B. Wang, M. Lin, and C. Liu, "On the secrecy performance of random VLC networks with imperfect CSI and protected zone," *IEEE Systems Journal*, vol. 14, no. 3, pp. 4176–4187, 2020.

[24] X. T. Fu, R. R. Lu, S. H. Lin, and J. Y. Wang, "Average channel capacity analysis for visible light communications with random receivers," in *2020 International Conference on Wireless Communications and Signal Processing (WCSP)*, 2020, pp. 331–336.

[25] *LUXEON Rebel Automotive*, Lumileds, 2020.

[26] Z. Ghassemlooy, W. Popoola, and S. Rajbhandari, *Optical wireless communications: system and channel modelling with MATLAB.* CRC press, 2019.

[27] B. S. a. Kerner, *Introduction to Modern Traffic Flow Theory and Control The Long Road to Three-Phase Traffic Theory*, 1st ed. Springer Science & Business Media, 2009.

[28] S. Abuelenin and A. Abul-Magd, "Empirical study of traffic velocity distribution and its effect on VANETs connectivity," in *Proc. 2014 ICCVE*, Nov 2014, pp. 391 – 395.

[29] Highways England. Site data tools.

[30] R. Nagel, "The effect of vehicular distance distributions and mobility on VANET communications," in *2010 IEEE Intelligent Vehicles Symposium*, June 2010, pp. 1190–1194.

[31] A. Papoulis and S. U. Pillai, *Probability, random variables, and stochastic processes.* Tata McGraw-Hill Education, 2002.

[32] D. Pal and C. Mallikarjuna, "Cellular automata cell structure for modeling heterogeneous traffic," *European Transport Trasporti Europei*, vol. 45, pp. 50–63, 08 2010.

[33] D. Pal and M. Chunchu, "Modeling of lateral gap maintaining behavior of vehicles in heterogeneous traffic stream," *Transportation Letters*, vol. 11, no. 7, pp. 373–381, 2019.

[34] J. Wang, K. Li, and X.-Y. Lu, "Chapter 5 - effect of human factors on driver behavior," in *Advances in Intelligent Vehicles*, Y. Chen and L. Li, Eds. Boston: Academic Press, 2014, pp. 111 – 157.

[35] J. Ben-Arie, "Image processing operators and transforms generated by a set of multidimensional neural lattices that use the central limit," in *Proc. 1991 IEEE IJCNN*, 1991, pp. 987–993 vol.2.

[36] I. S. Gradshtein and I. M. Ryzhik, *Table of integrals, series and products*, 7th ed. Amsterdam ; Boston: Elsevier, 2007.